Contribution from the Departments of Chemistry, The Ohio State University, Columbus, Ohio 43210, and the University of Notre Dame, Notre Dame, Indiana 46556

Preparation and NMR Spectra of $B_5H_9Fe(CO)_3$, an Analogue of B_6H_{10}

S. G. SHORE,* J. D. RAGAINI, R. L. SMITH, C. E. COTTRELL, and T. P. FEHLNER*

Received August 31, 1978

Conditions are described for the preparation of $B_5H_9Fe(CO)_3$ from the copyrolysis of $Fe(CO)_5$ with B_5H_9 in a hot–cold reactor, and mechanistic aspects of the reaction are presented and discussed. NMR spectra of $B_5H_9Fe(CO)_3$ are consistent with a pentagonal-pyramidal structure with the $Fe(CO)_3$ group located at a basal vertex site. There is a bridge hydrogen between iron and a basal boron atom which is fluxional. It moves between the two basal Fe–B sites. Carbonyl groups on iron are also fluxional. Rates for the proton exchanging between these Fe–B sites and carbonyl axial–equatorial interchange appear to be similar. From a line-shape analysis of the ^{13}C NMR spectra, the activation parameters $\Delta H^{\ddagger} = 12.7$ kcal/mol and $\Delta S^{\ddagger} = 11$ cal/(deg mol) were obtained.

Introduction

The ferraboranes $Fe(CO)_3B_5H_9$,[1] $Fe(CO)_5B_5H_3$,[2] and $Fe(CO)_3B_4H_8$[3] have been isolated from the copyrolysis of B_5H_9 with $Fe(CO)_5$. These structural and electronic analogues of the boron hydrides B_6H_{10},[4] $B_6H_{10}^{2-}$, and B_5H_9[5] are among a growing number of iron derivatives of boron hydride systems which have been prepared in recent years.[6] In addition to our preliminary report[2] of $Fe(CO)_3B_5H_9$ and $Fe(CO)_3B_5H_8^-$ its congugate base, the photoelectron spectrum of $Fe(CO)_3B_5H_9$ has been subsequently examined in detail,[7] and more recently the preparation and structure of the derivative $Cu[P(C_6H_5)_3]_2B_5H_8Fe(CO)_3$[8] was described. We present here details for the synthesis of $Fe(CO)_3B_5H_9$, describe some properties of the compound, present and discuss the results of an NMR investigation into the dynamic character of this analogue of hexaborane(10), and present and discuss some mechanistic apsects of the reaction of B_5H_9 with $Fe(CO)_5$.

Experimental Section

Methods. Standard vacuum line techniques were employed.[9]

Materials. Pentaborane(9) was obtained from the Callery Chemical Company, Callery, PA 16024, and iron pentacarbonyl was obtained from Alfa Products, Ventron Corp., Danvers, MA 01923. These materials were used as received.

NMR Spectra. Boron-11 and proton NMR spectra were recorded on a Varian HA-100 high-resolution NMR spectrometer at 32.1 MHz operating in the HR mode and 100 MHz in the HA mode, respectively. Decoupling equipment has been previously described.[10] Carbon-13 NMR spectra were recorded on a Brucker HX-90 spectrometer operating in the FT mode at 22.6 MHz.

Preparation of $B_5H_9Fe(CO)_3$. The preparation of $B_5H_9Fe(CO)_3$ was carried out in a hot–cold reactor which was constructed of Pyrex glass (Figure 1). This vessel was charged with 20 mmol of B_5H_9 and 20 mmol of $Fe(CO)_5$. The inner tube of the reactor was filled with sand which was heated to 230 or 260 °C by a resistance heater while the outer tube was immersed in a water bath at 25 °C. Every 24 h the reactants were cooled to −196 °C and noncondensable gas was pumped away, and the reaction was allowed to continue. When the temperature of the inner tube was kept at 230 °C, the reaction was allowed to proceed for 4–5 days. A reaction period of 1–2 days was employed when the inner tube was kept at 260 °C. Under each set of conditions the yield of $Fe(CO)_3B_5H_9$ was approximately 1 mmol. At the conclusion of a reaction the condensable components were distilled out of the reactor and passed through U-traps at 0 and −35 °C and into a trap at −196 °C. Decaborane(14) which is formed as a byproduct of the reaction was retained in the trap at 0 °C while $Fe(CO)_3B_5H_9$ was retained in the trap at −35 °C.

Caution. The Pyrex hot–cold reactor exhibited signs of structural weakness after extended use. Etching and splintering of the glass occurred. Frequent inspection of the reactor is mandatory in order to ensure the safety of personnel. Under the reaction conditions described above, in which the hot portion of the reactor was kept at 230 °C, 4 months was the maximum cumulative time in service before replacement of the reactor. When the inner tube was kept at 260 °C, the reactor was replaced at the first indication of etching of the glass, usually after 6 reactions.

Kinetic Study. The kinetic study of the copyrolysis of B_5H_9 and $Fe(CO)_5$ was carried out in the Pyrex reactor portrayed in Figure 2. The reactor was directly coupled to an AEI MS 902 high-resolution mass spectrometer via the small, thin-walled Pyrex orifice indicated in the figure, thereby allowing the composition of the system to be monitored continuously as a function of time. The size of the leak was chosen such that the first-order rate coefficient for loss of material through the leak was small compared to the loss of reactants due to chemical reaction. Calibration of the leak was carried out using argon. The reactor proper was heated resistively, and the temperature was monitored by means of a thermocouple. The reactor volume was 100 mL, and after the first run the internal surfaces of the reactor were coated with a black, metallic film which probably was iron. In order to match the conditions in the hot-cold reactor as closely as possible, the reactor was charged with vapor from a liquid mixture of B_5H_9 and $Fe(CO)_5$ held at 25 °C. Under these conditions the pressure of B_5H_9 is about 200 torr and that of $Fe(CO)_5$ is 10 times smaller. No other gas was added so that the total pressure was about 220 torr. Relative composition was measured by monitoring appropriate ion intensities. The composition of the only ferraborane product observed in the kinetic study, $B_4H_8Fe(CO)_3$, was confirmed by precise mass measurements as $^{11}B_4{}^1H_8{}^{12}C_3{}^{16}O_3{}^{56}Fe$ (obsd 192.019 amu; calcd 192.019 amu). Mixing was by diffusion as no provision for external mixing was made.

Results and Discussion

Preparation. Under the conditions given above, for the hot–cold reactor, the yield of $B_5H_9Fe(CO)_3$ is maximized. There is no evidence for the formation of $B_4H_8Fe(CO)_3$ observable by NMR spectra. If the noncondensable gases are not periodically removed from the reactor, then some $B_4H_8Fe(CO)_3$ is formed as well.

The product $B_5H_9Fe(CO)_3$ is a deep red, mobile liquid at room temperature with a vapor pressure of less than 1 torr. It flashes in the presence of oxygen. In the absence of air no decomposition is observed after 30 min at room temperature. Pyrolysis of $B_5H_9Fe(CO)_3$ at 110 °C for a period of 6 h gives 30% conversion to $B_4H_8Fe(CO)_3$. Under fluorescent lights and irradiation at 360 nm, $B_5H_9Fe(CO)_3$ decomposes slowly. Extended exposure results in the formation of a dark brown scum, even when the sample has been kept at −78 °C.

The mass spectrum of $B_5H_9Fe(CO)_3$ is typical of a molecule that contains a metal carbonyl fragment. The high-mass cutoff is *m/e* 204, and major fragment ions corresponding to the loss of three CO molecules are observed. Relative intensity distributions of the parent ion cluster and those fragments due to loss of CO were characteristic of a compound containing five boron atoms (obsd 87:100:59:21; calcd 80:100:49:12). Significant hydrogen fragmentation is observed only for the $B_5H_9Fe^+$ ion and those of lower mass. This suggests the absence of terminal hydrogens on the iron atom.[11] Precise mass measurements on the *m/e* 204 ion yielded a composition of $^{11}B_5{}^1H_9{}^{12}C_3{}^{16}O_3{}^{56}Fe$ (obsd 204.036 ± 0.002 amu; calcd

---

* To whom correspondence should be addressed: S.G.S., The Ohio State University; T.P.F., University of Notre Dame.

0020-1669/79/1318-0670$01.00/0

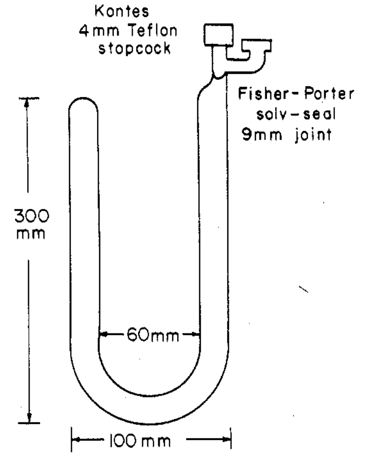

Figure 1. Pyrex hot–cold reactor used for synthesis of $B_5H_9Fe(CO)_3$.

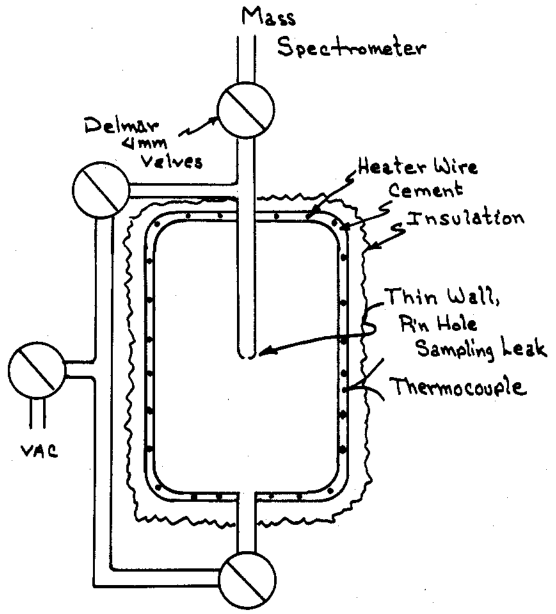

Figure 2. Pyrex hot–cold reactor used to examine the copyrolysis of B_5H_9 and $Fe(CO)_5$. The reactor volume is 100 mL.

204.037 amu). X-ray structure determinations of the derivatives $[N(n\text{-}C_4H_9)_4][B_5H_8Fe(CO)_3]^2$ and $Cu[P(C_6H_5)_3]_2B_5H_8Fe(CO)_3{}^8$ establish the parent cluster to be a pentagonal pyramid with the $Fe(CO)_3$ unit at a basal site with a bridging hydrogen between iron and an adjacent boron atom.

NMR Spectra. Boron-11, proton, and carbon-13 NMR spectra (Table I, Figures 3 and 4) reveal $B_5H_9Fe(CO)_3$ to be a fluxional molecule with respect to the bridging proton between iron and boron and with respect to the carbonyl groups on iron. At 25 °C, the boron-11 NMR spectrum (Figure 3) of $B_5H_9Fe(CO)_3$ consists of two sets of doublets (relative areas 2:2) which can be assigned to the basal boron atoms and a high-field doublet which is assigned to the apical boron. The doublet character of each signal arises from spin coupling of each terminal hydrogen with the boron atom to which it is bound. Proton decoupling causes each doublet to collapse to a singlet. When the temperature is lowered (−80 °C), each basal signal splits into two resonances, thus revealing five separate boron resonances which are expected from a slowly exchanging (on the boron-11 NMR time scale) or static system which is asymmetric.

Table I. NMR Data

boron-11[a]

		−80 °C δ, ppm	25 °C δ, ppm	J_{BH}, Hz
B_1		−47.0	−47.4	140
B_4 or B_5		2.3		
	(7.9)		8.2	150
B_5 or B_4		13.5		
B_6		37.7		
	(46.3)		46.0	150
B_3		55.5		

proton[b]

		−80 °C δ, ppm	25 °C δ, ppm
Fe–H–B		−16.79	
H_1		−1.22	−1.19
H_μ		−0.72	
H_μ	(0.06)	0.08	0.10
H_μ		0.82	
H_5 or H_4		3.86	
	(4.20)		4.19
H_5 or H_4		4.53	
H_6		5.97	
	(6.41)		6.40
H_3		6.84	

carbon-13[c]

	−120 °C δ, ppm	−30 °C δ, ppm
	210.5	
(207.9)	207.7	208.3
	206.6	

[a] In CH_2Cl_2 solution. $\delta_{BF_3\cdot O(C_2H_5)_2} = 0$ ppm. A positive shift indicates a resonance downfield from the reference $BF_3\cdot O(C_2H_5)_2$. See *J. Organomet. Chem.*, **131**, C43 (1977). [b] In CH_2Cl_2 solution. $\delta_{Me_4Si} = 0$ ppm. [c] In $(CD_3)_2O$ solution. $\delta_{Me_4Si} = 0$ ppm.

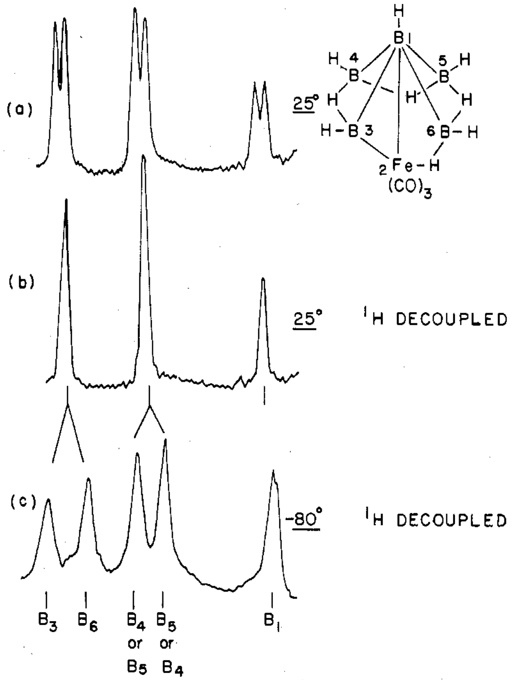

Figure 3. Boron-11 NMR spectra of $B_5H_9Fe(CO)_3$ in $(CD_3)_2O$.

The proton NMR spectrum (boron-11 decoupled) (Figure 4) at 25 °C reveals a signal at high field which is assigned to the hydrogen in the Fe–H–B bond. The single signal assigned to the three B–H–B hydrogens and the two signals assigned to the terminal hydrogens on basal boron atoms are consistent with a fluxional system. As the temperature is lowered, each of the resonances assigned to basal terminal hydrogens splits into two resonances, and the signal from the bridge protons splits into three resonances. At −80 °C the nine individual

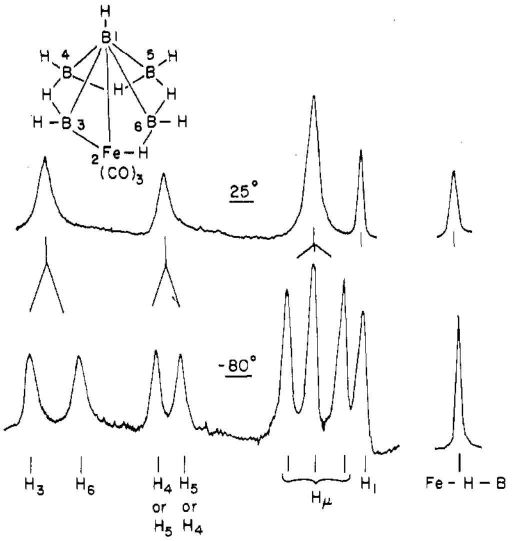

Figure 4. Proton NMR spectra of $B_5H_9Fe(CO)_3$.

proton resonances of $B_5H_9Fe(CO)_3$ are observed. This spectrum reflects a static structure which is asymmetric which is consistent with the X-ray results.[2] From selective decoupling experiments, the assignments H_3, H_6 and B_3, B_6 were made. The resonance of the hydrogen in the Fe–H–B bond and the resonance assigned to H_6 are noticeably sharpened when a decoupling frequency consistent for B_6 is employed. Conversely, only the resonance assigned to H_3 is noticeably sharpened when a decoupling frequency consistent for B_3 is employed. The sharpening of the resonance assigned to Fe–H–B upon boron-11 spin-decoupling is consistent with the existence of a three-center Fe–H–B bond.

The fluxional character of $B_5H_9Fe(CO)_3$ most likely arises from movement of the H atom in the Fe–H–B bridge between the two possible bridging sites. The constancy of the chemical shift of this hydrogen as the temperature is changed indicates that there is no mixing with other hydrogens in the molecule. Indeed, it is not necessary to assume that the hydrogens in the B–H–B bonds are fluxional. Their resonances are averaged by the fluxional behavior of the Fe–H–B hydrogen. In the exchange process between sites, this hydrogen is apparently always bound to iron, and the breaking of the Fe–H–B bond occurs as Fe–H|B rather than breaking as metal|H–B which is commonly observed in other fluxional metalloboranes.[12]

The $Fe(CO)_3$ group is also fluxional (see Table I). Carbon-13 NMR spectra were recorded over the temperature range −100 to −30 °C. At −100 °C three carbonyl resonances were observed. As the temperature was raised, the transitions broadened, coalesced, and sharpened to a single, sharp line at −30 °C. Simulated spectra for a three-site exchange process were calculated,[13] and an Eyring plot of the rate constants obtained by matching theoretical and experimental spectra gave $\Delta H^{\ddagger} = 12.7$ kcal/mol and $\Delta S^{\ddagger} = 11$ cal/(deg mol). Although a line-shape analysis was not performed on the proton spectra, measurements of coalescence points gave rates which were similar to those observed in the carbon-13 NMR spectra.

Kinetic Study. In order to gain some insight into the process by which ferraboranes are generated in the copyrolysis of B_5H_9 and $Fe(CO)_5$, a semiquantitative study of the pyrolytic system under the conditions that obtain in the hot–cold reactor was carried out using the reactor described in the Experimental Section. Typical data are shown in Figure 5 in which the decay of $Fe(CO)_5$ and formation of $Fe(CO)_3B_4H_8$ are shown as a function of time at a reactor temperature of 217 °C. The decay of B_5H_9 was also monitored; however, since it was present in tenfold excess, it remained essentially constant over the period of measurement. No evidence for the presence of any other ferraboranes was found, and it should also be noted that $Fe(CO)_3B_4H_8$ reached a level of about 0.2% of the B_5H_9 present. Note that the sampling configuration only allows the detection of compounds that are relatively stable under the reaction condition. Pyrolysis at 204 °C of a mixture of $Fe(CO)_3B_4H_8$ and $Fe(CO)_3B_5H_9$ resulted in the rapid destruction of the latter while the former was essentially unaffected over the period of 1 h. Clearly then, $Fe(CO)_3B_4H_8$ is the most stable ferraborane produced and, in the absence of the cold surface of the hot–cold reactor, is the only ferraborane observed. The fact that $B_5H_9Fe(CO)_3$ is the major ferraborane observed in the hot–cold reactor described above demonstrates that $B_5H_9Fe(CO)_3$ is formed before $B_4H_8Fe(CO)_3$ in the copyrolysis of B_5H_9 and $Fe(CO)_5$.

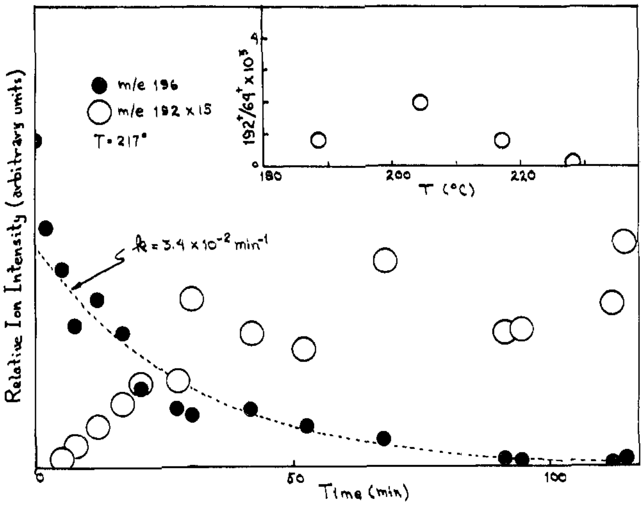

Figure 5. Typical kinetic data showing the loss of $Fe(CO)_5$ represented by the relative intensity of *m/e* 196 and the formation of $Fe(CO)_3B_4H_8$ represented by the relative intensity of *m/e* 192. The inset shows the relative yield of $B_4H_8Fe(CO)_3$ with respect to B_5H_9 (*m/e* 64) as a function of wall temperature.

The data on the decay of $Fe(CO)_5$ as a function of time at various temperatures were fitted to exponentrial decay curves as indicated in the example in Figure 5 and the first order rate coefficients thus obtained. Although the fit was reasonable ($r^2 = 0.92$), the data were not good enough to unambiguously establish the reaction order. The temperature dependence of the first-order rate constants yields an activation energy of about 35 kcal/mol. This is consistent with a rate-determining Fe–C bond cleavage for which the average bond energy is estimated to be 28 kcal.[14] The data on $B_4H_8Fe(CO)_3$ are only used to demonstrate the formation of this compound as a product and the relative proportion of this product in the reaction mixture.

As shown in the inset of Figure 5, the yield of $B_4H_8Fe(CO)_3$ reaches a maximum at a reactor temperature of about 200 °C. As the rate of decay of B_5H_9 is considerably less than that of $Fe(CO)_5$ over the temperature range studied, we suggest that the increase in yield to the maximum from lower temperature is due to the increase in the rate of $Fe(CO)_5$ decomposition (see above) while the decrease from the maximum as the temperature is raised further is due to decomposition of $B_4H_8Fe(CO)_3$. In turn, this suggests that it is the decomposition of $Fe(CO)_5$ that initiates the formation of the ferraboranes, probably by the scission of the Fe–C bond. The fact that the yield of $B_4H_8Fe(CO)_3$ at any time is much less than the loss of $Fe(CO)_5$ requires a parallel path for the loss of $Fe(CO)_5$. Thus we suggest that the initial steps of the copyrolysis are

$$Fe(CO)_5 \rightarrow Fe(CO)_4 + CO$$

$$Fe(CO)_4 \xrightarrow{\text{wall}} Fe + 4CO$$

$$Fe(CO)_4 + B_5H_9 \rightarrow \text{ferraboranes}$$

As demonstrated with the hot–cold reactor, the initial ferraborane produced in the pyrolysis is $B_5H_9Fe(CO)_3$. Thus, we also write

$$Fe(CO)_4 + B_5H_9 \rightarrow B_5H_9Fe(CO)_3 + CO$$

Finally, the other ferraboranes that have been observed in this system may well be produced by the subsequent decomposition of $B_5H_9Fe(CO)_3$. For example, since $Fe(CO)_3B_5H_9$ is known to produce $Fe(CO)_3B_4H_8$ on heating (see above) and since nido heteroboranes are known to disproportionate,[15] the following reaction may take place:

$$2Fe(CO)_3B_5H_9 \rightarrow Fe(CO)_3B_4H_8 + Fe(CO)_3B_6H_{10}$$

The latter product, which is an analogue of B_7H_{11} (a very unstable borane),[16] may well decompose and, thus, contribute to the substantial amount of intractable material formed in the system.

These results allow one to explain the fact that the reported preparations of both $Fe(CO)_3B_4H_8$[3] and $Fe(CO)_3B_5H_9$[2] use essentially the same type of hot–cold pyrolytic reactor. Clearly, the ferraborane observed as product will depend on the net effectiveness of trapping at the cold surface. This in turn depends on the distance between hot and cold surfaces *and* the mean free path, i.e., the pressure. Reactor geometry is important, but, in addition, in this particular reaction as considerable quantities of CO are produced, the pressure in the reactor rises with time thereby decreasing the mean free path and effectiveness of trapping. Thus, removal of the CO enhances formation of $Fe(CO)_3B_5H_9$ while letting the pressure build up results in formation of the more stable $Fe(CO)_3B_4H_8$.

Acknowledgment. We thank the National Science Foundation for support of this work through Grants CHE76-18705 and CHE75-1908. We also thank Drs. G. Frankel and J. M. Geckle for a copy of the line-shape program used.

Registry No. $B_5H_9Fe(CO)_3$, 61403-41-6; $Fe(CO)_5$, 13463-40-6; B_5H_9, 19624-22-7.

References and Notes

(1) T. P. Fehlner, J. Ragaini, M. Mangion, and S. G. Shore, *J. Am. Chem. Soc.*, **98**, 7085 (1976).
(2) J. A. Ulman and T. P. Fehlner, *J. Chem. Soc., Chem. Commun.*, 632 (1976).
(3) N. N. Greenwood, C. G. Savory, R. N. Grimes, L. G. Sneddon, A. Davison, and S. S. Wreford, *J. Chem. Soc., Chem. Commun.*, 718 (1974).
(4) Other analogues of B_6H_{10} are known: $(\eta^5\text{-}C_5H_5)FeB_5H_{10}$ isomers, R. Weiss and R. N. Grimes, *J. Am. Chem. Soc.*, **99**, 8087 (1977); $Mn(CO)_3B_5H_{10}$, M. B. Fischer, D. F. Gaines, and J. D. Kessler, Abstracts, 174th National Meeting of the American Chemical Society, Chicago, IL, Sept 1977, No. INOR 167.
(5) Other analogues of B_5H_9 are isomeric species of composition $(\eta^5\text{-}C_5H_5)CoB_4H_8$: V. R. Miller and R. N. Grimes, *J. Am. Chem. Soc.*, **95**, 5078 (1973); L. G. Sneddon and D. Voet, *J. Chem. Soc., Chem. Commun.*, 118 (1976); V. R. Miller, R. Weiss, and R. N. Grimes, *J. Am. Chem. Soc.*, **99**, 5646 (1977); R. Weiss, J. B. Bowser, and R. N. Grimes, *Inorg. Chem.*, **17**, 1522 (1978).
(6) Among the other ferraboranes reported are the following: $\mu\text{-}Fe(CO)_4B_2H_5^-$, G. Medford and S. G. Shore, *J. Am. Chem. Soc.*, **100**, 3953 (1978); $\mu\text{-}Fe(CO)_4B_6H_{10}$, A. Davison, D. D. Traficante, and S. S. Wreford, *ibid.*, **96**, 2802 (1974); $\mu\text{-}Fe(CO)_4B_7H_{12}^-$, O. Hollander, W. R. Clayton, and S. G. Shore, *J. Chem. Soc., Chem. Commun.*, 605 (1974), and M. Mangion, W. R. Clayton, O. Hollander, and S. G. Shore, *Inorg. Chem.*, **16**, 2110 (1977); two $Fe\text{–}Be_3H_8$ compounds, D. F. Gaines and S. Hildebrandt, *ibid.*, **17**, 794 (1978); $Fe_2(CO)_6B_2H_6$, E. L. Andersen and T. P. Fehlner, *J. Am. Chem. Soc.*, **100**, 4606 (1978).
(7) J. A. Ulman, E. L. Andersen, and T. P. Fehlner, *J. Am. Chem. Soc.*, **100**, 456 (1978).
(8) M. Mangion, J. D. Ragaini, T. Schmitkons, and S. G. Shore, *J. Am. Chem. Soc.*, in press.
(9) D. F. Shriver, "The Manipulation of Air-Sensitive Compounds", McGraw-Hill, New York, 1969.
(10) V. T. Brice, H. D. Johnson, II, and S. G. Shore, *J. Am. Chem. Soc.*, **95**, 6629 (1973).
(11) G. L. Geoffroy and J. R. Lehman, *Adv. Inorg. Chem. Radiochem.*, **19**, 198 (1977).
(12) H. Beal and C. H. Bushweller, *Chem. Rev.*, **73**, 465 (1973).
(13) J. I. Kaplan and G. Fraenkel, *J. Am. Chem. Soc.*, **94**, 2907 (1972), and references cited therein.
(14) F. A. Cotton, A. K. Fischer, and G. Wilkinson, *J. Am. Chem. Soc.*, **81**, 800 (1959).
(15) T. Onak, "Boron Hydrides", E. L. Muetterties, Ed., Academic Press, New York, 1975, Chapter 10.
(16) W. N. Lipscomb, "Boron Hydrides", W. A. Benjamin, New York, 1963.

Contribution from the Institute of Industrial Science,
University of Tokyo, Minatoku, Tokyo, Japan

^1H, ^{13}C, and ^{195}Pt Nuclear Magnetic Resonance Studies on Diastereomeric Platinum(II) Complexes of Prochiral Olefins Containing a Chiral Amino Acid Ligand

SUMIO SHINODA, YOSHIHARU YAMAGUCHI, and YASUKAZU SAITO*

Received June 9, 1978

The nature of diastereomeric discrimination in the series of platinum(II) complexes *trans*(*N*,olefin)-chloro(*N*-methyl-(*S*)-prolinato)(olefin)platinum (olefin = propene, *trans*-2-butene, *tert*-butylethylene, styrene, *p*-chlorostyrene, or *p*-methoxystyrene) has been investigated by using ^1H, ^{13}C, and ^{195}Pt nuclear magnetic resonance. The observed trend of diastereomeric difference in the NMR properties (especially $^1J_{PtC}$ for coordinated carbons and δ_{Pt}) indicated that the abundant diastereomers had a stronger platinum–olefin bonding, and thus enhanced thermodynamic stability. Contrasting NMR features found for the styrene and *tert*-butylethylene diastereomers are interpreted in terms of a different mode of distortion of coordinated olefins upon complex formation.

Introduction

Enantioface differentiation[1] in the η^2 coordination of prochiral olefins to chiral metallic species often forms a key step for asymmetric syntheses with olefinic compounds used as sources.[2] Because of quite high stability, platinum(II)–olefin complexes have been utilized as a suitable model for studying the stereoselectivity in this step in the presence of an optically active ligand.[3]

Since NMR spectroscopy is useful for the analysis of molecular structures in solutions or the elucidation of bonding characteristics of molecules, detailed examination of various NMR properties should afford a precise description of the nature of diastereomeric molecules. As far as coordination compounds are concerned, platinum is one of the most favorable metals for this purpose, because extra information on nuclear spin coupling is obtainable by virtue of the presence of a ^{195}Pt nucleus ($I = {}^1/_2$, natural abundance 33.8%).

In the present paper, ^1H, ^{13}C, and ^{195}Pt NMR data have been collected for a number of diastereomeric platinum(II)–olefin complexes and combined to study (i) their solution